Generation of ionospheric ducts by the HAARP HF heater

2010 Phys. Scr. 2010 014040

(http://iopscience.iop.org/1402-4896/2010/T142/014040)

IOP PUBLISHING PHYSICA SCRIPTA

Phys. Scr. **T142** (2010) 014040 (7pp) doi:10.1088/0031-8949/2010/T142/014040

Generation of ionospheric ducts by the HAARP HF heater

J A Cohen[1], R Pradipta[1], L M Burton[1], A Labno[1], M C Lee[1,2], B J Watkins[3], C Fallen[3], S P Kuo[4], W J Burke[5], D Mabius[2] and B Z See[2]

[1] Massachusetts Institute of Technology, Cambridge, MA 02139, USA
[2] Boston University, Boston, MA 02215, USA
[3] University of Alaska Fairbanks, Fairbanks, AK 99775, USA
[4] New York University, Brooklyn, NY 11201, USA
[5] Air Force Research Laboratory, Hanscom AFB, MA 01731, USA

E-mail: mclee@mit.edu

Received 8 July 2010
Accepted for publication 23 August 2010
Published 31 December 2010
Online at stacks.iop.org/PhysScr/T142/014040

Abstract
We report an investigation of ionospheric ducts having the shape of large plasma sheets, generated by vertically transmitted HAARP HF heater waves in several experiments conducted in Gakona, Alaska. Theory predicts that O-mode heater wave-created ionospheric ducts form parallel-plate waveguides within the meridional plane, and those generated by the X-mode heater waves are orthogonal to the meridional plane. Our theoretical prediction is supported by measurements of ionosonde data (namely ionograms), range–time–intensity (RTI) plots of UHF and HF backscatter radars, as well as magnetometer data analyses. When these plasma sheets experienced $\mathbf{E} \times \mathbf{B}$ drifts, they were intercepted by the HAARP UHF radar and seen as slanted stripes in the RTI plots. This striking feature was also observed in our earlier experiments using the Arecibo UHF radar.

PACS numbers: 94.20.−y, 94.05.−a

(Some figures in this article are in colour only in the electronic version.)

1. Introduction

We have been conducting experiments in Gakona, Alaska to investigate the characteristic features of HAARP HF heater-induced large-scale ionospheric ducts (Cohen *et al* 2008) as well as short-scale plasma waves (Burton *et al* 2008). Depending on the polarizations (i.e. O-mode or X-mode) of the heater waves, these large-scale ionospheric plasma structures have different configurations. In brief, large-scale sheet-like ionospheric density irregularities can be excited within and orthogonal to meridional planes above Gakona by vertically injected O-mode and X-mode heater waves, respectively, as illustrated in figures 1 and 2 (Cohen *et al* 2008, Kuo *et al* 2009 and references therein). How these plasma sheets can affect ionosonde signals in the presence of distant plasma blobs, as delineated in figures 1 and 2, will be discussed in the next section.

These experiments were motivated by our earlier Arecibo experiments, wherein we observed HF heater-generated large plasma sheets (Lee *et al* 1998). Presented in figure 3 is a range–time–intensity (RTI) plot of Arecibo 430 MHz backscattered radar echoes, showing that large sheet-like plasma density irregularities were created by Arecibo O-mode HF heater waves within the meridional planes. When these plasma sheets experienced $\mathbf{E} \times \mathbf{B}$ drifts, they were detected by the Arecibo radar and were seen as slanted stripes in the RTI plots. These large plasma sheets, known as 'artificial ionospheric ducts' or 'waveguides', had successfully supported the US Navy Naval transmitter (codenamed NAU)-launched 28.5 kHz whistler waves to propagate between Arecibo, Puerto Rico and Trelew, Argentina along the $L = 1.35$ magnetic flux tube (Starks and Lee 2000, Starks *et al* 2001, Pradipta *et al* 2008). This work has important applications for radiation belt remediation

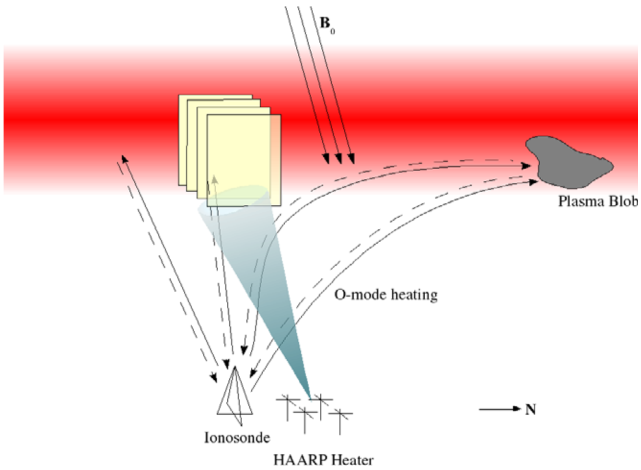

Figure 1. Large plasma sheets generated by O-mode HAARP heater waves within the meridional plane. Ionosonde signals can be bounced back by remote plasma blobs to propagate through those parallel-plate waveguides and recorded in ionograms.

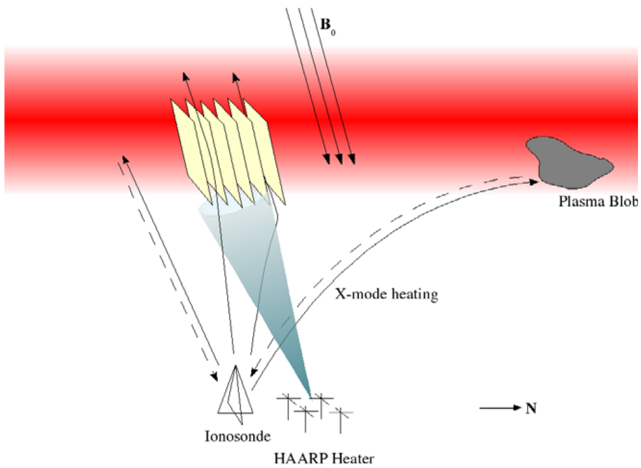

Figure 2. Large plasma sheets generated by X-mode HAARP heater waves are orthogonal to the meridional plane. Ionosonde signals transmitted near the zenith will be guided by these plasma sheets to propagate away. Thus they cannot be bounced back to appear in the ionograms. However, ionosonde signals transmitted at large angles from the zenith can still be reflected by remote plasma blobs and recorded in ionograms.

(Pradipta *et al* 2007) and whistler wave interactions with ionospheric plasmas (Labno *et al* 2007).

2. Detection of heater-excited large plasma sheets at the HAARP facility

Several diagnostic instruments have been used to detect HAARP heater-generated large plasma sheets, including an ionosonde, MUIR (Modular UHF Ionospheric Radar at 446 MHz), SuperDARN HF backscatter radar and magnetometers. The results are discussed as follows.

2.1. Digisonde measurements

We use a sequence of ionograms, displayed in figure 4, to discuss the effects of HF heater-excited plasma irregularities on signals transmitted from the HAARP ionosonde. In the

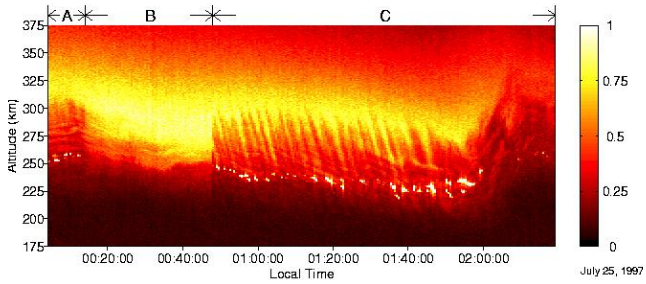

Figure 3. Arecibo radar detection of O-mode HF heater wave-created large plasma sheets (seen on the RTI plot as slanted stripes), from about 00:50 to 01:50 LT on 25 July 1997 (Lee *et al* 1998).

attached color code, O+ and O− denote the blueshifted and redshifted return echoes of ordinary ionosonde signals from the vertical direction, respectively. Similarly, X+ and X− denote the blueshifted and redshifted return echoes of extraordinary ionosonde signals from the vertical direction, respectively. Other colors denote echoes from the oblique direction (indicated by NNE, E, W, SSW, SSE, NNW) without Doppler information.

These representative ionograms were recorded during our experiments conducted on 21 August 2005 from 10:00 UT to 12:15 UT. Prior to our experiments, ionogram (a) (figure 4(a)) was recorded at 9:55 UT during the vertical transmission of ramped X-mode. The ionograms showed strong spread-F and ionosonde signals were reflected from the northward direction. Our experiments began with 3.16 MHz CW O-mode transmitted along the magnetic zenith. As soon as the heater was switched to this mode, a vertical stripe appeared around the heater frequency, affecting the blue northward traces (ionogram (b)). This reduction in signal persisted throughout the O-mode heating. When the heater was turned off, the traces filled in again (ionogram (c)).

The heater was turned on at 11:05:30, transmitting 3.15 MHz CW X-mode vertically. A decrease in northward signal intensity was again seen, but was more pronounced this time (ionogram (d)). Changing the heater direction to the magnetic zenith did not make an appreciable difference (ionogram (e)), but increasing the heater frequency to 4.50 MHz at 11:35:30 altered the appearance of the ionograms. A vertical stripe appeared around the new heater frequency, but was narrower and bore greater resemblance to the first O-mode stripe in ionogram (b), centered in a narrow frequency range around the heater frequency (ionogram (f)). At this higher frequency, there was not a significant difference when we switched to CW O-mode, still transmitting at 4.50 MHz (ionogram (g)). Increasing the frequency once more and transmitting 6.80 MHz CW O-mode had no apparent effect on the ionogram traces and they filled back in quickly (ionogram (h)). When the heater was turned off, the traces remained essentially the same (ionogram (i)). We note that there was an apparent weakening of the X-mode trace on the ionograms when the heater began transmitting CW X-mode (ionogram (d)) and in fact this trace disappeared altogether after 5 min. However, when the heater was later switched to CW O-mode (ionograms (g) and (h)) and eventually turned off (ionograms (i)), the X-mode trace did become apparent

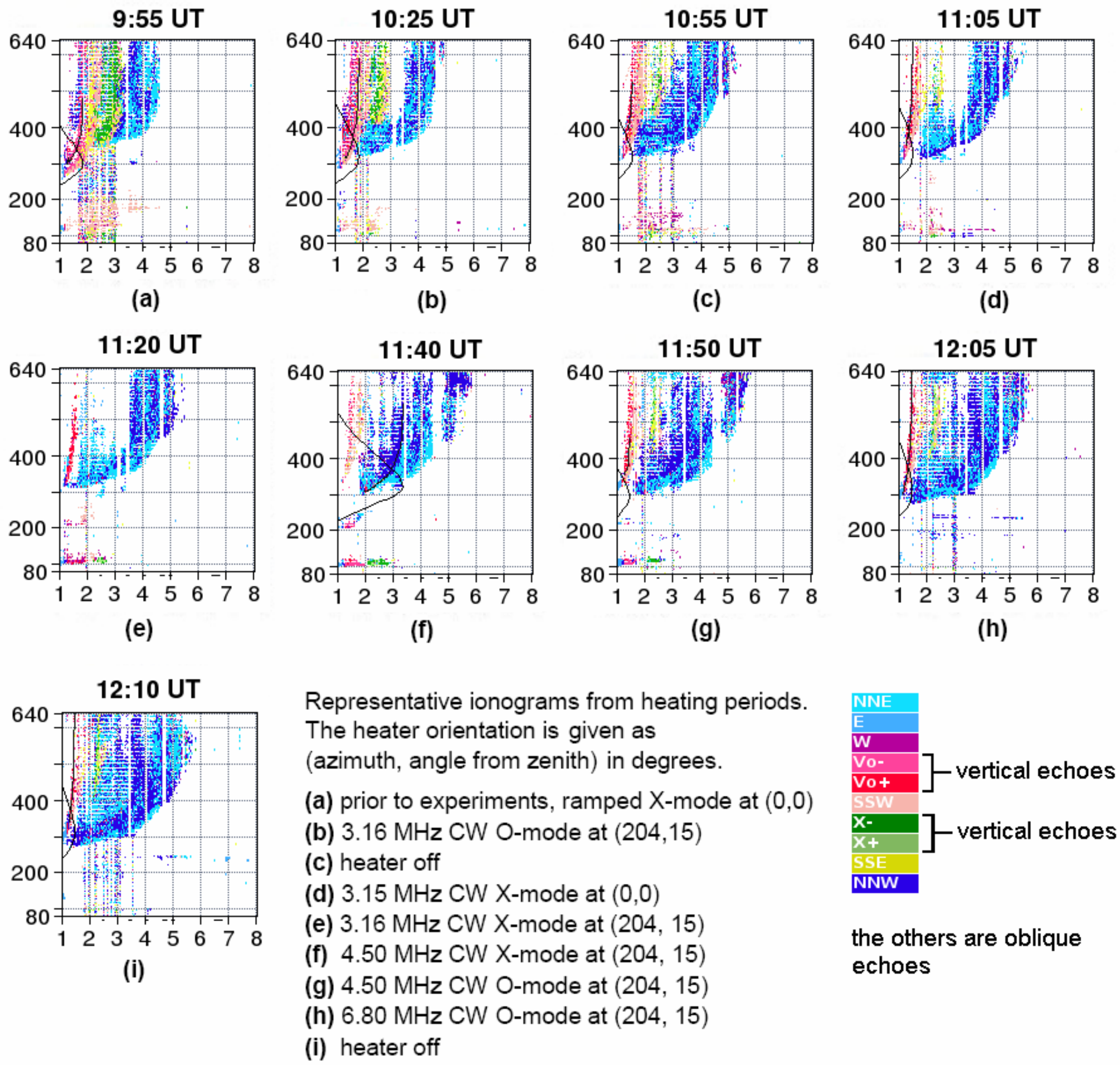

Figure 4. Ionograms recorded in HAARP experiments on 21 August 2005.

again. Thus, it is interesting to examine what effect the heater had on the X-mode trace in ionograms.

We expect that heater-excited small-scale and large-scale irregularities may scatter and duct ionosonde signals, respectively, and cause a loss in received signal near the heater frequency (Kuo *et al* 2009). This results in the appearance of broad vertical stripes in ionograms. While narrow stripes may be automatically taken out by the ionosonde software, namely automatic gain control (Reinisch 2009), the stripes in ionograms show rough edges, which are not characteristic of software-removed interference lines. In addition, we believe that heater-excited large plasma sheets are responsible for the reduction of northward signals in the ionograms. During the night of our experiments on 21 August 2005, a plasma blob was seen in total electron content (TEC) measurements to the north of HAARP (see figure 5), taken by a LEO receiver with the right geometry to produce a tomographic image of electron density over Alaska.

As shown in figure 1, CW O-mode heating produces sheet-like irregularities parallel to the meridional plane. Ionosonde signals that are refracted by the ionosphere may reach and be reflected by the density gradient created by the plasma blob. These reflected signals reaching the ionosonde are seen as blue northward traces. There existed some correlation between ionospheric structures such as plasma blobs and the intense northward traces. As illustrated in figure 2, CW X-mode heating produces sheet-like irregularities that are perpendicular to the meridional plane. In this scenario, the ionosonde signals that would otherwise be reflected by the plasma blob are ducted away or undergo scattering. This interpretation provides a plausible explanation regarding HAARP heater effects on the observed X-mode trace in concerned ionograms.

2.2. MUIR and SuperDARN radar measurements

The aforementioned effects of excited plasma density irregularities on HAARP digisonde have also been seen on

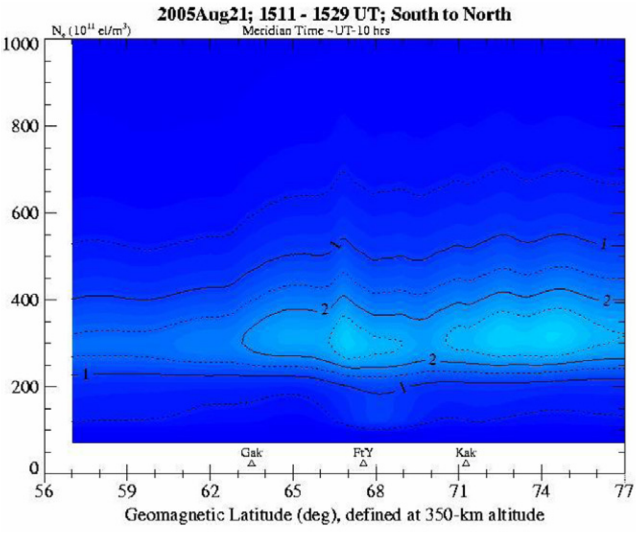

Figure 5. TEC measurements from LEO satellites over Alaska on 21 August 2008 from 15:11 to 15:29 UT.

the operation of MUIR and SuperDARN radar. MUIR is not as sensitive as the Arecibo radar. Thus, Arecibo radar measurements to generate RTI of electron density structures, as shown in figure 3, cannot be done by MUIR. However, the RTI plots of ion lines can be produced by MUIR. Displayed in figure 6 is such an RTI plot of MUIR ion line measurements recorded from 01:43:00 to 01:59:30 UT on 21 October 2009. It shows that three large sheet-like plasma density irregularities were created by HAARP O-mode HF heater waves within the meridional planes, and detected by MUIR from 01:49 to 01:54 UT. When these plasma sheets experienced $\mathbf{E} \times \mathbf{B}$ drifts, they were intercepted by MUIR radar and are seen as slanted stripes in the RTI plots.

By contrast, the RTI plot of SuperDARN backscatter radar measurements that is displayed in figure 7 shows different aspects but expected features of plasma sheets, which were generated by vertically transmitted heater waves during our HAARP experiment on 27 February 2008. In these experiments Kodiak SuperDARN radar periodically scanned the region overhead HAARP (beam no. 8). The range is about 670 km for the SuperDARN beam to reach the heated ionospheric region above Gakona. It is seen from the RTI plot that SuperDARN signals weakened significantly when we changed the heating schemes from O-mode to X-mode. We have used black arrows in the RTI plot to show the significant reduction of radar echo occurring during CW X-mode operation. This feature is consistent with the measurements using SuperDARN beam no. 2, which scanned the west side of the heated region to diagnose drifted away large plasma structures. That is, radar echoes from X-mode excited plasma structures were significantly weaker than those from O-mode excited structures. During the O-mode heating SuperDARN signals were bounced back by plasma sheets generated within the meridional plane, as shown in figure 1. By contrast, SuperDARN signals were forward-scattered by X-mode generated plasma sheets, which are orthogonal to the meridional plane as illustrated in figure 2. These scenarios explain reasonably well why the SuperDARN signals weakened significantly when we changed the heating schemes from O-mode to X-mode.

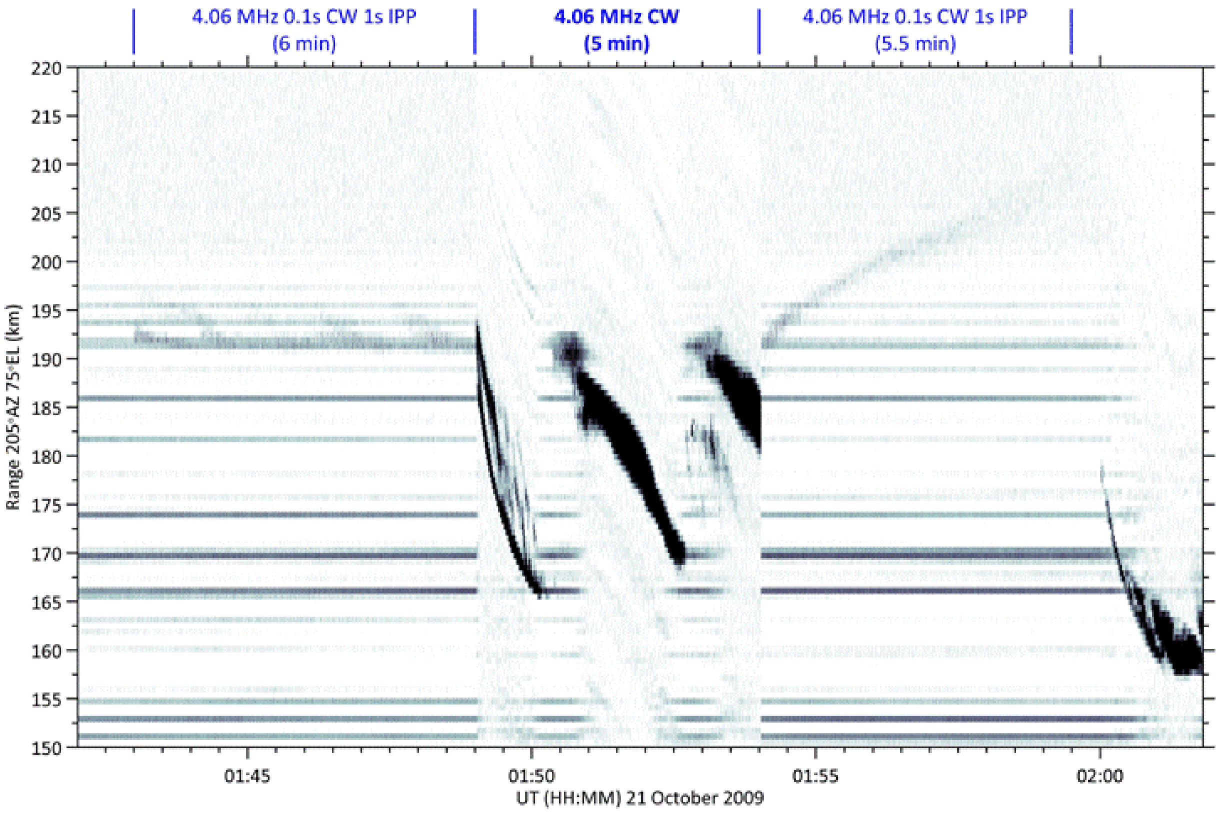

Figure 6. HAARP MUIR radar detection of O-mode HF heater wave-created large plasma sheets (seen on RTI plot as slanted stripes), from about 01:49 to 01:54 UT on 21 October 2009 (Fallen 2009).

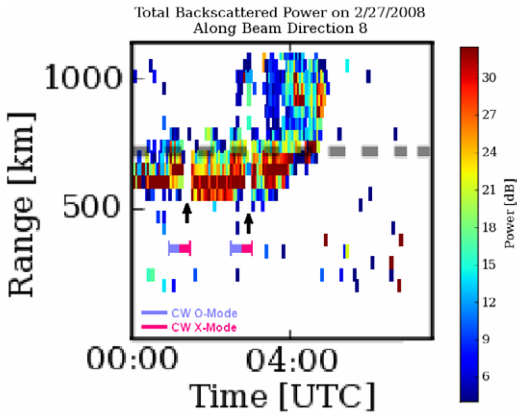

Figure 7. SuperDARN data recorded during CW O-mode and CW X-mode operation of the HAARP heater on 27 February 2008 for the investigation of the generation of large plasma sheets.

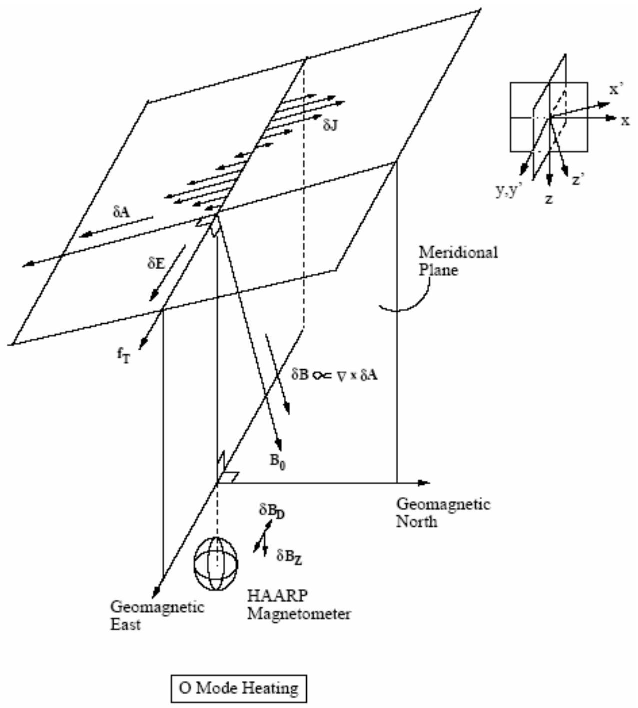

Figure 8. Simultaneous generation of plasma density fluctuations (δn) and geomagnetic fluctuations ($\boldsymbol{\delta}\mathbf{B}$) in O-mode HF heating experiments (adapted from Lee and Kuo 1985).

2.3. Magnetometer measurements

HF heater wave-excited 'thermal filamentation instability' is responsible for the generation of ionospheric ducts in the form of large plasma sheets. A striking feature of this mechanism is the simultaneous generation of plasma density fluctuations (δn) and geomagnetic fluctuations ($\boldsymbol{\delta}\mathbf{B}$) (Kuo *et al* 2009 and references therein). This physical process is briefly described as follows with the aid of figures 8 and 9 (adapted from Lee and Kuo 1985). Differential joule heating, resulting from the interactions of HF heater waves and excited high-frequency sidebands, yields a thermal pressure force ($\mathbf{f_T}$) on electrons across the geomagnetic field, pointing to the direction along the y-axis ('Geomagnetic East' as specified in figure 8 for O-mode heating) or along the x-axis ('Geomagnetic North

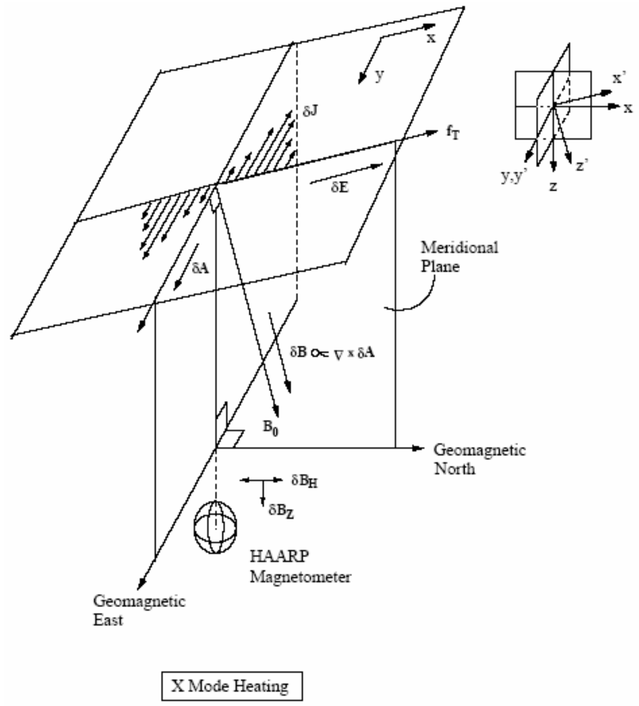

Figure 9. Simultaneous generation of plasma density fluctuations (δn) and geomagnetic fluctuations ($\boldsymbol{\delta}\mathbf{B}$) in X-mode HF heating experiments (adapted from Lee and Kuo 1985).

and upward' as specified in figure 9 for X-mode heating). Note that the thermal pressure force ($\mathbf{f_T}$) gives rise to electron density fluctuations (δn) with wave vectors ($\mathbf{k}$) pointing along the same direction. Hence, large plasma sheets are produced within (or orthogonal to) the meridional plane for the O-mode (X-mode) heating cases, as vividly illustrated in figures 8 and 9, respectively.

The thermal pressure force ($\mathbf{f_T}$) leads to an $\mathbf{f_T} \times \mathbf{B_0}$ drift motion of electrons and, consequently, induces a net electron drift current along the x-axis (as shown in figure 8 for O-mode heating) or along the y-axis (as shown in figure 9 for X-mode heating). The direction of the current is perpendicular to both the background magnetic field B_0 and the wave vector $\mathbf{k}$ of the excited plasma density irregularities. Therefore, magnetic field fluctuations ($\boldsymbol{\delta}\mathbf{B}$) are excited along the background Earth's magnetic field ($\mathbf{B_0}$ designated as the z-axis) simultaneously with the density irregularities via the filamentation instability in both O- and X-mode heating processes. Note that the background geomagnetic field ($\mathbf{B_0}$) has a dip angle of 75.8°. Thus, it has three components (designated as $\mathbf{B_{0D}}$, $\mathbf{B_{0H}}$ and $\mathbf{B_{0Z}}$) along the East–West, North–South and downward directions, respectively. Therefore, the excited magnetic field fluctuations ($\boldsymbol{\delta}\mathbf{B}$) also have the corresponding three components (designated as $\boldsymbol{\delta}\mathbf{B_D}$, $\boldsymbol{\delta}\mathbf{B_H}$ and $\boldsymbol{\delta}\mathbf{B_Z}$).

Based on our theoretical analyses and illustrations of the simultaneous excitations of δn and $\boldsymbol{\delta}\mathbf{B}$ in figures 8 and 9, aided by the delineation of sheet-like configurations in figures 1 and 2, we can expect that $\boldsymbol{\delta}\mathbf{B_D}$ and $\boldsymbol{\delta}\mathbf{B_Z}$ (or $\boldsymbol{\delta}\mathbf{B_H}$ and $\boldsymbol{\delta}\mathbf{B_Z}$) will be highly correlated in O-mode (or X-mode) heating experiments. While our detailed correlation study of these magnetic field fluctuations is in progress, we present in figure 10 the preliminary correlation analyses: the η_{HZ} of $\boldsymbol{\delta}\mathbf{B_H}$

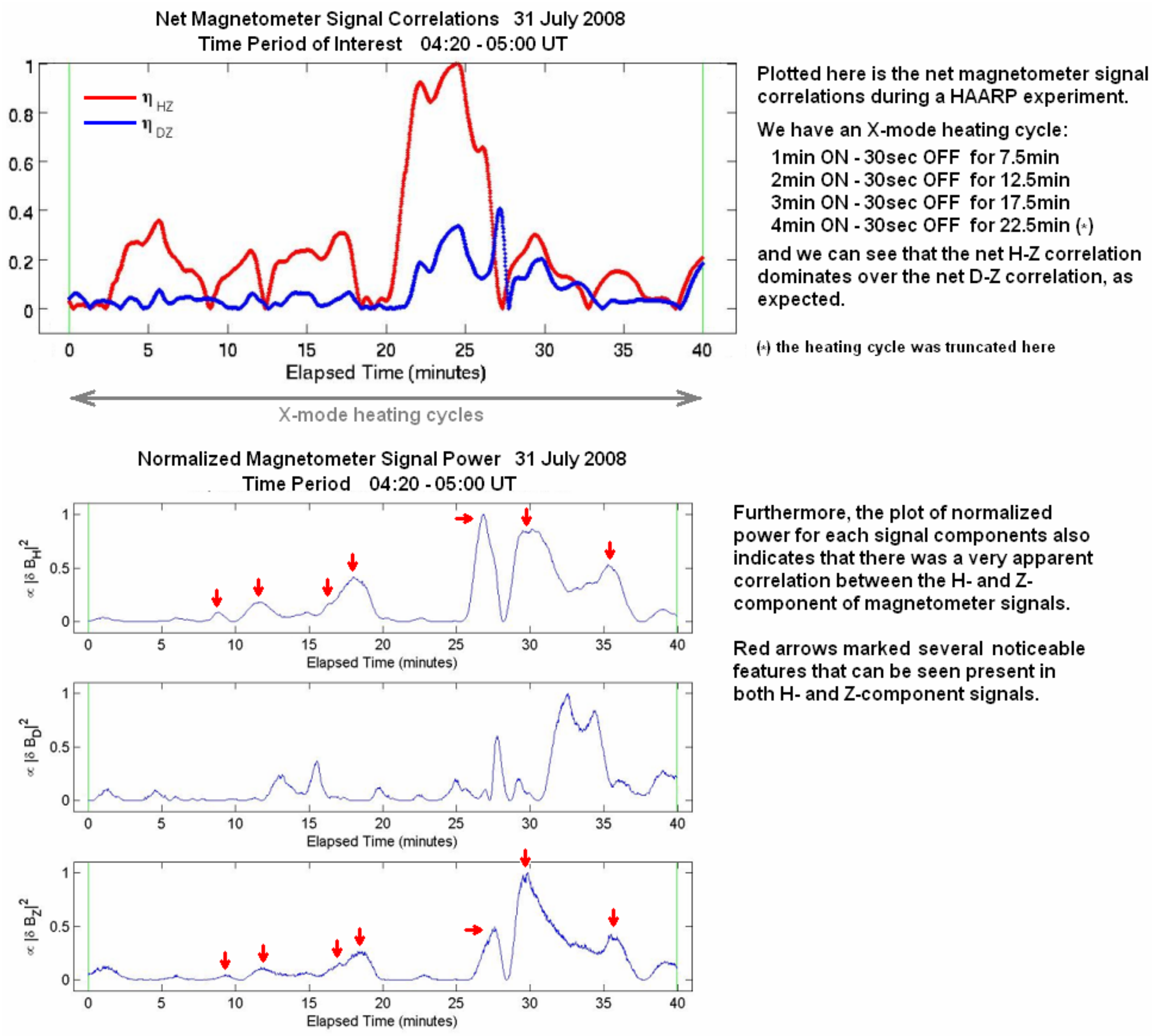

Figure 10. Generation of large plasma sheets by X-mode heater waves supported by close correlation of excited $\boldsymbol{\delta}\mathbf{B_H}$ and $\boldsymbol{\delta}\mathbf{B_Z}$ (in red) (top panel) and temporal power variation of $\mu|\delta B_H|^2$ and $\mu|\delta B_Z|^2$.

and $\boldsymbol{\delta}\mathbf{B_Z}$ and the η_{DZ} of $\boldsymbol{\delta}\mathbf{B_D}$ and $\boldsymbol{\delta}\mathbf{B_Z}$ (top panel) and a plot of normalized power for $\boldsymbol{\delta}\mathbf{B_D}$, $\boldsymbol{\delta}\mathbf{B_H}$, and $\boldsymbol{\delta}\mathbf{B_Z}$ (bottom panel).

It is seen in figure 10 that during the X-mode heating experiments carried out on 31 July 2008, the η_{HZ} of $\boldsymbol{\delta}\mathbf{B_H}$ and $\boldsymbol{\delta}\mathbf{B_Z}$ (in red) is much greater than the η_{DZ} of $\boldsymbol{\delta}\mathbf{B_D}$ and $\boldsymbol{\delta}\mathbf{B_Z}$ (in blue). This indicates that large plasma sheets orthogonal to the meridional plane were favorably excited by X-mode heater waves, as elaborated above. This is further supported by the temporal variations of the normalized power $\mu|\delta B_H|^2$ and $\mu|\delta B_Z|^2$, which show very similar patterns and features, as marked by red arrows in the bottom panel of figure 10.

3. Summary and discussions

We present the data recorded by several HAARP experiments in Gakona, Alaska aimed at investigating HF heater wave-induced ionospheric ducts for radiation belt remediation, controlled study of space plasma turbulence and communications, etc. These artificial ionospheric ducts are sheet-like large-scale plasma irregularities (δn), excited by O-mode and X-mode HF heater waves via thermal filamentation instabilities within and orthogonal to meridional planes, respectively. The configurations of these plasma sheets are supported by HAARP digisonde data (namely ionograms), as well as MUIR radar and SuperDARN radar signals due to reflection and scattering off the plasma sheets. When these plasma sheets experienced $E \times B$ drifts, they were intercepted by MUIR radar and are seen as slanted stripes in the RTI plots. A similar striking feature was seen in our Arecibo experiments. Our preliminary magnetometer data analysis confirms the characteristic features of the simultaneously excited geomagnetic field fluctuations ($\boldsymbol{\delta}\mathbf{B}$), reflecting the geometry of the plasma sheets. For example, close correlation between $\boldsymbol{\delta}\mathbf{B_H}$ and $\boldsymbol{\delta}\mathbf{B_Z}$ is indeed found for X-mode generated plasma sheets, expected to be orthogonal to the meridional plane.

Acknowledgment

This work was supported by the HAARP under ONR grants N00014-07-1-0999 (MIT), ONR-N00014-10-1-0856 (NYU) and N00014-17-1-1082 (UAF). We thank Bodo Reinisch, Dima Paznukhov, Lee Snyder and Mike McCarrick for useful discussions and Bill Bristow and Jeff Spaleta for providing SuperDARN data. A part of this paper was presented by MCL as an invited lecture at the 2nd International Conference and Advanced School on 'Turbulent Mixing and Beyond', held at the International Centre for Theoretical Physics, 27 July–7 August 2009, Trieste, Italy.

References

Burton L M, Cohen J A, Pradipta R, Labno A, Lee M C, Batishchev O, Rokusek D L, Kuo S P, Watkins B J and Oyama S 2008 Excitation and diagnosis of cascading Langmuir waves in ionospheric plasmas at Gakona, Alaska *Phys. Scr.* **T132** 014030

Cohen J A, Burton L M, Pradipta R, Labno A, Lee MC, Kuo S P, Watkins B J and Oyama S 2008 Ionospheric ducts and plasma waves induced by HF heater over Gakona *Proc. XXIX URSI General Assembly (Chicago, IL, 7–16 August 2008)*

Fallen C T 2010 Applications of a time-dependent polar ionosphere model for radio modification experiments *PhD Thesis* University of Alaska Fairbanks, Fairbanks

Kuo S P, Cheng W-T, Cohen J A, Pradipta R, Lee M C, Kuo S S and Snyder A 2009 Simultaneous generation of large-scale density irregularities and geomagnetic pulsations via filamentation instability *Geophys. Res. Lett.* **36** L09107

Labno A, Pradipta R, Lee M C, Sulzer M P, Burton L M, Cohen J A, Kuo S P and Rokusek D L 2007 Whistler-mode wave interactions with ionospheric plasmas over Arecibo *J. Geophys. Res.* **112** A03306

Lee M C and Kuo S P 1985 Simultaneous excitation of large-scale geomagnetic field fluctuations and plasma density irregularities by powerful radio waves *Radio Sci.* **20** 539

Lee M C, Riddolls R J, Burke W J, Sulzer M P, Kuo S P and Klien E M C 1998 Generation of large sheet-like ionospheric plasma irregularities at Arecibo *Geophys. Res. Lett.* **25** 3067

Pradipta R, Labno A, Lee M C, Burke W J, Sulzer M P, Cohen J A, Burton L M, Kuo S P and Rokusek D L 2007 Electron precipitation from the inner radiation belt above Arecibo *Geophys. Res. Lett.* **34** L08101

Pradipta R *et al* 2008 Space plasma disturbances caused by launched whistler waves *Phys. Scr.* **T132** 014031

Reinisch B 2009 private communication

Starks M J and Lee M C 2000 Matched filtering for the measurement of conjugately ducted VLF transmission *Radio Sci.* **35** 351

Starks M J, Lee M C and Jastrzebski P 2001 Interhemispheric propagation of VLF transmissions in the presence of ionospheric HF heating *J. Geophys. Res.* **106** 5579